EUROPHYSICS LETTERS 1 March 2004

Europhys. Lett., **65** (5), pp. 671–677 (2004)
DOI: 10.1209/epl/i2003-10176-1

Finite-size effects on surface segregation in polymer blend films above and below the critical point of phase separation

H. Grüll[1,2](*), L. Sung[1], A. Karim[1], J. F. Douglas[1](**), S. K. Satija[1], M. Hayashi[3], H. Jinnai[3], T. Hashimoto[3] and C. C. Han[1]

[1] *Material Science and Engineering Laboratory, National Institute of Standards and Technology (NIST) - Gaithersburg, MD 20899-8542, USA*
[2] *Philips Research - 5656 AA Eindhoven, The Netherlands*
[3] *Department of Polymer Chemistry, Graduate School of Engineering Kyoto University - Kyoto 606-8501, Japan*

(received 26 August 2003; accepted in final form 5 January 2004)

PACS. 61.12.Ha – Neutron reflectometry.
PACS. 68.08.Bc – Wetting.
PACS. 05.70.Fh – Phase transitions: general studies.

Abstract. – We investigate the influence of temperature and confinement on surface segregation in thin films of deuterated polybutadiene and polyisoprene near the critical point for phase separation. Neutron reflectivity measurements show that polyisoprene enriches at the air and silicon interfaces in both the 1- and 2-phase regions. A transition between in-plane and surface-directed (layered) phase separation is observed with increasing film thickness. Weak critical adsorption effects cause the blend composition profile to be rounded in comparison with profiles normally measured in small liquid mixtures.

Fluid mixtures near the critical point for phase separation are characteristically sensitive to perturbations because of the vanishing interfacial tension between the coexisting phases. This often leads to the formation of enrichment layers near interacting boundaries which have important ramifications for multi-phase flow in porous media [1], the stability and transport of colloid particles in binary fluids [2] or filled multiphase polymeric systems [3]. The thickness of compositional enrichment layers, ξ_s, formed at interacting boundaries is expected to increase sharply near the critical point [4]. It is often assumed that ξ_s has a similar temperature dependence to the bulk correlation length of concentration fluctuations ($\xi_b \sim \xi_s$), leading to a divergence of ξ_s near the critical point in semi-infinite systems. It has also been suggested that the liquid-surface interaction can limit the growth of ξ_s [5]. However, the investigation of this question is limited to very thick films as ξ_s must remain finite in thin films.

Boundary interactions have a large impact on the morphology of thin blend films. In the case where each polymer segregates to one of the boundaries (asymmetric segregation)

(*) E-mail: holger.gruell@philips.com
(**) E-mail: jack.douglas@nist.gov

the coexisting phases arrange in a bilayer structure [6, 7]. In the case where one component segregates to both interfaces (symmetric segregation) [8–11], the film morphology depends additionally on the film thickness. Thicker films stay smooth and it was suggested that these films show a trilayer-type structure [9–11]. For films with a thickness smaller than a characteristic length L_c on the order of the interfacial width in bulk, there is the possibility for a phase separation within the film middle layer triggering a surface "roughening" [10, 11]. Recent simulations suggest that thin films confined by symmetric boundaries (*e.g.*, two identical walls) will exhibit also this type of in-plane phase separation [12]. In the present paper, we investigate this possibility directly by neutron reflectivity (NR).

NR is used to determine the depth profile of a partially miscible binary polymer blend thin film of poly(isoprene) (PI) and deuterated poly(butadiene) (dPB) as a function of film thickness d and temperature T near the critical point for phase separation. The blend dPB/PI showed, in earlier experiments [13], symmetrical segregation of PI for asymmetric confinement (Si and air). The depth profile allows for extracting the surface enrichment length, ξ_s, and the surface excess, z^*_{PI}, of the preferentially adsorbing polymer at the polymer-air and the polymer-Si interface.

The bulk phase behavior of the blend dPB ($M_w = 104\,\mathrm{kg/mol}$; $M_w/M_n = 1.06$) and PI ($M_w = 142\,\mathrm{kg/mol}$; $M_w/M_n = 1.03$) was studied by small-angle neutron scattering [14]. This blend shows a lower critical-solution–type phase behavior (LCST) with a bulk critical temperature $T_{c,b} = 54.5 \pm 1\,^\circ\mathrm{C}$ and a critical volume fraction of dPB $\phi_c^{dPB} = 0.552 \pm 0.001$. The Flory-Huggins parameter [15] χ_{FH} and the bulk correlation length ξ_b were determined as $\chi_{FH}(T) = 0.00541\text{–}1.4234/T$ and $\xi_b = \xi_\circ \cdot \epsilon^{-0.504\pm0.008}$, where $\epsilon = (T_c - T)/T_c$ and $\xi_\circ = 3.36 \pm 0.09\,\mathrm{nm}$. Uniform polymer blend films with different thicknesses d ($400 < d/\,\text{Å} < 1700$), of dPB/PI with near-critical composition were spin-coated from toluene on Si wafers of 5 mm thickness and 75 mm diameter. The film thickness was determined using X-ray reflectivity measurements. Prior to spin-coating, the Si substrates were cleaned by boiling in a bath of $H_2O/30\%NH_3/30\%\text{-}H_2O_2$ (5:1:1 by vol.) and then by boiling in concentrated $H_2SO_4/30\%\text{-}H_2O_2$ (7:3, 1 h, $T = 80\,^\circ\mathrm{C}$). The Si-oxide layer was stripped using a buffered 3% HF solution for 2 min and regrown by a 3 min irradiation with ultraviolet light. Neutron reflectivity measurements were performed at NIST Center for Neutron Research, Gaithersburg, MD. The measurements were taken inside a heatable vacuum chamber at a reduced pressure of 10^{-6} Pa with 2 h equilibration at each temperature. Repeated measurements over 16 h showed no further changes in the reflectivity. The film roughness was determined by AFM and X-ray reflectivity. Freshly cast polymer films show a RMS roughness of $\sigma \simeq 5\,\text{Å}$, which increases slightly upon annealing to $\sigma \simeq 12\,\text{Å}$. After background subtraction, the neutron reflectivity data were fit using a standard multilayer fitting routine [16]. As neutron reflectivity averages the signal over the coherence length of the neutron beam of the order of several microns, compositional inhomogeneities within the plane of the film are averaged. All NR data can be consistently fit by using stretched exponential functions of the form $\psi(z) = (b/v)_s^{air,Si} + [(b/v)_c - (b/v)_s^{air,Si}] \cdot \exp[-(z/\ell_s^{air,Si})^{\beta^{air,Si}}]$ to model the scattering length density (SLD) change from each interface towards the film center. $(b/v)_s^{air,Si}$ is the SLD at the air and Si interface, respectively, with $\ell_s^{air,Si}$ as the decay length and $\beta^{air,Si}$ as the exponent. The functional form of "stretched exponential" profile is motivated by the decay of the order parameter in an Ising model with a long-range surface interaction [17], but the exponent was taken to be adjustable. Although these standard NR measurements do not provide a unique information about the functional form of the SLD profile, the stretched exponential functional fit all data best taking χ^2 as a measure in comparison with other tested functions. The model functions used here are consistent with the absolute measurement of the composition profile in a film of the same polymer blend system using polarized neutron

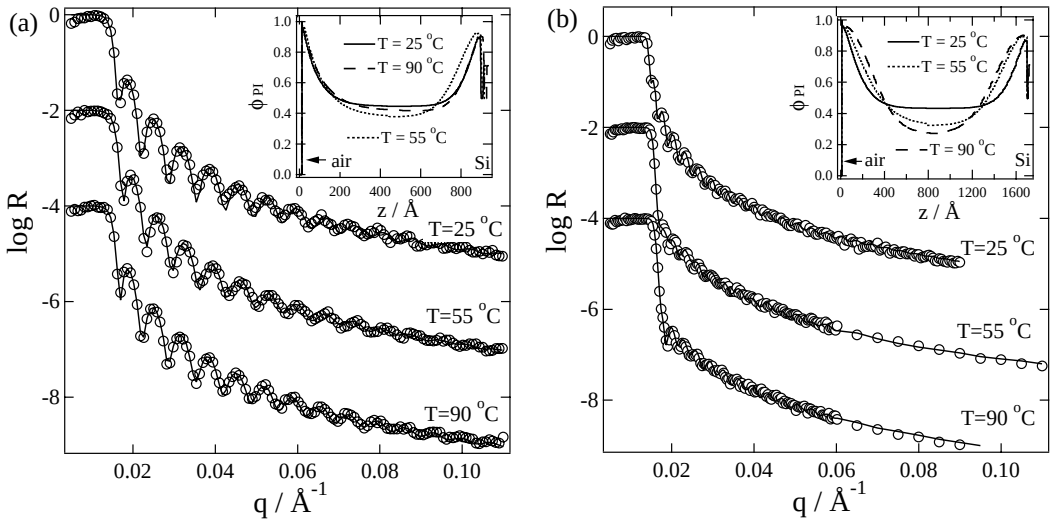

Fig. 1 – Neutron reflectivity data for three different temperatures taken with films of different thicknesses: (a) $d = 890$ Å and (b) $d = 1680$ Å. At lower q ($q \leq 0.08$ Å^{-1}) the standard deviation is smaller than the symbol size, at highest q it corresponds to half a decade on the log scale at the most. The ϕ-model profiles used to fit the data are shown in the insets.

reflectivity [13]. The SLD profiles are converted to composition profiles using the relation $\psi(z) = (b/v)_{\mathrm{dPB}} \cdot \phi_{\mathrm{dPB}} + (b/v)_{\mathrm{PI}} \cdot \phi_{\mathrm{PI}}$ ($\phi_{\mathrm{PI}} + \phi_{\mathrm{dPB}} = 1$ and $(b/v)_{\mathrm{dPB}} = 6.64 \cdot 10^{-6}$ Å^{-2}; $(b/v)_{\mathrm{PI}} = 0.26 \cdot 10^{-6}$ Å^{-2}). The thickness of the adsorbed PI layer at the air and Si interface is evaluated by calculating the surface enrichment length ξ_{s}, defined as the second moment of the interfacial profile [18], $\xi_{\mathrm{s}} = \sqrt{\langle z^2 \rangle} = ([\int_0^\infty z^2 \exp[-(z/\ell_{\mathrm{s}})^\beta]\mathrm{d}z]/[\int_0^\infty \exp[-(z/\ell_{\mathrm{s}})^\beta]\mathrm{d}z])^{1/2}$.

Figure 1 shows typical NR data and composition profiles $\phi(z)$ for two different film thicknesses (a) $d = 890$ Å and (b) $d = 1685$ Å at three different temperatures that correspond to a temperature in the 1-phase region, the critical temperature of bulk phase separation, $T_{\mathrm{c,b}}$, and a temperature inside the 2-phase region of the bulk mixture. All composition profiles show a strong PI segregation to the air and Si interface, independent of film thickness and temperature. Due to the strong segregation of PI to both interfaces, a depletion of PI in the film center (*i.e.* enrichment of dPB) is observed leading to a trilayer structure and a symmetric film profile. The composition profile in a 700 Å film at $T = 25\,^{\circ}$C can be described with individual single exponential functions ($\beta = 1$) for each interface, consistent with earlier findings [13]. However, we find that the exponent β as well as the decay length ℓ_{s} for both interfaces increase systematically with increasing film thickness and temperature. Notably, the composition profiles of the thicker films ($d > 1200$ Å) at $T = 90\,^{\circ}$C are considerably "rounded" at the interfaces, giving an exponent $\beta \simeq 2$ (see figs. 1(a) and (b)). We will discuss the rounded shape of the adsorption profile in detail later. The temperature evolution of the composition profile for films thinner than about 1200 Å is considerably different from thicker films. Upon approaching $T_{\mathrm{c,b}}$ from the 1-phase, PI increasingly enriches at both interfaces, thus increasing ξ_{s} (fig. 2), together with a further dPB enrichment in the film center (fig. 3(a)). Upon entering the bulk 2-phase region, this trend reverses for films with $d < 1200$ Å: the profile at $T = 90\,^{\circ}$C is very similar to the profile at $T = 25\,^{\circ}$C (fig. 1(a)). Films with $d > 1200$ Å behave the opposite way as an increasing PI segregation to both interfaces is observed for temperatures above the critical temperature of bulk-phase separation, $T > T_{\mathrm{c,b}}$ (fig. 1(b)).

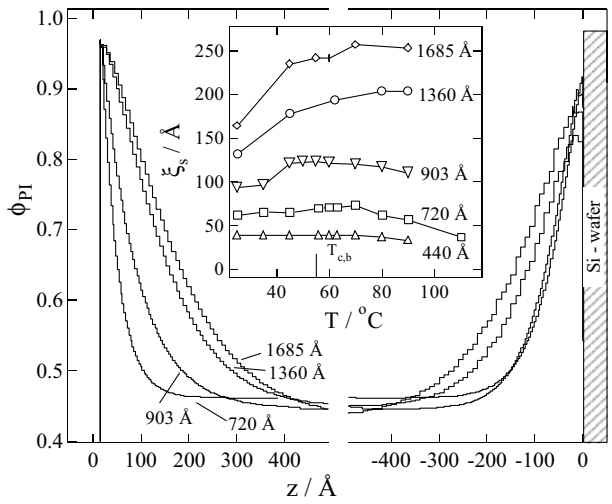

Fig. 2 – Surface enrichment layers at the air and Si interface in films of different thicknesses. The averaged surface enrichment length $\xi_s = (\xi_s^{air} + \xi_s^{Si})/2$ is shown in the inset.

Figure 2 shows the composition profiles for films of different thickness at $T = 25\,^{\circ}\mathrm{C}$. Decreasing the film thickness obviously leads to a "squeezing" of the surface enrichment layer, *i.e.* $\beta \to 1$ and a decrease of ℓ_s, but no significant change of the PI volume fraction ϕ_s right at the polymer/air and polymer/Si interface occurs. The surface enrichment lengths of PI for the air and Si side, ξ_s^{air} and ξ_s^{Si}, have similar values and vary similarly with T and d. As the fit parameters, β, ℓ_s, for the Si and air interface are slightly coupled, the average of both surface enrichment lengths, $\xi_s = (\xi_s^{air} + \xi_s^{Si})/2$, is taken and shown in the inset of fig. 2. The scale of the PI enrichment becomes enhanced as $T_{c,b}$ is approached either from above or below for films with $d < 1200\,\text{Å}$. In thicker films, ξ_s grows with increasing temperature approaching $T_{c,b}$ and levels off entering the 2-phase region.

This temperature and film thickness dependence can be quantified from the volume fraction of dPB in the film center, ϕ_{cen}^{dPB}, shown in fig. 3(a) and the PI surface excess z_{PI}^* (fig. 3(b)) with $z_{PI}^* = \int_0^d [\phi_{PI}(z) - \phi_{cen}^{PI}]\mathrm{d}z$. Approaching the bulk binodal line clearly leads to an enrichment of dPB in the film center which reflects the build-up of a thick PI-rich adsorption layer at both interfaces with a thickness ξ_s. This effect becomes larger with increased film thickness and is similar to critical-adsorption experiments in small binary mixtures [19]. For a given temperature above the bulk critical temperature, ϕ_{cen}^{dPB} approaches the composition of the bulk coexisting dPB-rich phase with increasing film thickness, as can be seen in comparison to the binodal line. As neutron reflectivity averages the signal over the coherence length of the neutron beam of the order of several microns, compositional inhomogeneities within the plane of the film are averaged. The volume fraction ϕ_{cen}^{dPB} determined by NR represents therefore the laterally averaged volume fraction in the (x, y)-plane of the film. In the 2-phase region, the film is composed of domains in a volume ratio v of the two coexisting phases of the thin film $\phi_{cen}^{dPB} = v \cdot \phi_{coex}^{dPB\text{-rich}} + (1 - v) \cdot \phi_{coex}^{PI\text{-rich}}$, where $\phi_{coex}^{a,b}$ are given by the thin-film phase diagram [12]. We believe the tendency for ϕ_{cen} to become richer in dPB with increasing film thickness at a given temperature inside the 2-phase region reflects a change in volume ratio v due to gradual morphological transition from domains to layers rather than a change in the compositions of the coexisting phases ϕ_{coex}. Thus, a value of ϕ_{cen} close to the average

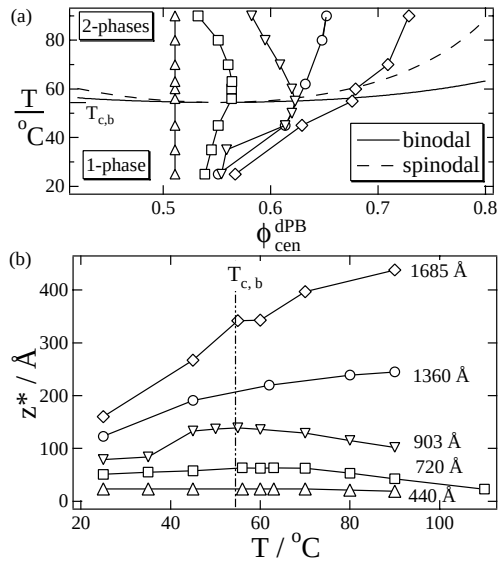

Fig. 3 – (a) Volume fraction of the film center $\phi_{\rm cen}^{\rm dPB}$ as a function of temperature for films with different thicknesses. The center volume fraction is an average volume fraction determined by the volume ratio of the two coexisting phases. (b) Sum of the surface excess, $z_{\rm PI}^*$, at the air and Si interface; error bars correspond to twice the symbol size.

composition, as observed in the very thin films, occurs when all inhomogeneities along the film center are composed of equal amounts of both coexisting phases ($v \simeq 0.5$). As both $\xi_{\rm s}$ and $\phi_{\rm cen}$ contribute to the surface excess, $z_{\rm PI}^*$ shows a similar, but more pronounced thickness and temperature dependence (fig. 3(b)).

The data in fig. 2 show that $\xi_{\rm s}$ increases for all film thicknesses upon approaching the bulk critical temperature, but remains finite near $T_{\rm c,b}$. Furthermore, the absence of any temperature dependence for $\xi_{\rm s}$ and $z_{\rm PI}^*$ in the film with $d = 440\,$Å reveals a strong finite-size effect on the phase behavior of polymer blend films. The above findings can be explained with a gradual change from an in-plane phase separation for thinner films to a more layered type morphology in thicker films. For films with $d < 1200\,$Å, an in-plane phase separation leads to $\phi_{\rm coex}^{\rm PI\text{-}rich}$ and $\phi_{\rm coex}^{\rm dPB\text{-}rich}$ domains inside the 2-phase region. The maximum of $z_{\rm PI}^*$ around the bulk critical temperature is caused by the maximum in $\xi_{\rm s}$, leading to a high enrichment of dPB in the film center. The film shows a more pronounced trilayer-type structure for T near $T_{\rm c}$. The decrease of $z_{\rm PI}^*$ upon further heating can be explained with the increasing interfacial tension between the two coexisting phases: It costs less energy to maintain this trilayer-type structure close to $T_{\rm c}$ than deeper inside the 2-phase region due to the vanishing interfacial tension at $T_{\rm c}$ according to $\gamma \sim \epsilon^{\mu}$ ($\epsilon = (T_{\rm c} - T)/T_{\rm c}$; $\mu \simeq 1.26$). Going deeper into the 2-phase region, γ increases and in thinner films it becomes energetically more favorable to form domains instead of maintaining the trilayer morphology. The total interfacial area A between the coexisting phases is minimized by forming interfaces perpendicular to the film surface. This interpretation is supported by recent simulations [12]. The almost linear increase of $z_{\rm PI}^*$ with temperatures above the critical point in films with $d > 1200\,$Å can be rationalized by assuming a more pronounced trilayer structure as the segregation power (χ) between the coexisting phases increases. This promotes a further segregation of the PI-rich phase to both interfaces with the dPB-rich phase located mostly in the film center. Thicker films are

less likely to form perpendicular interfaces in the 2-phase region as the gain in free energy, $\mathrm{d}G = \gamma \cdot \mathrm{d}A$, decreases with increasing film thickness. Furthermore, a trilayer structure is stabilized by strong surface interactions in such a way that composition waves extending from each wall constructively interact in thicker films. Thus, a thick film can exist in a metastable trilayer structure. These results contrast with recent findings in polymer films confined by weakly interacting walls [20].

The rounded shape of the adsorption profile at the polymer-air interface was observed before [21–23], and theory [24] as well as simulations [25] recently indicated the possibility of a rounded profile. We take this as evidence for a "weak critical adsorption" where the profile near the boundary is influenced by the polymer structure [5]. The polymer blend composition profiles, which we approximate by stretched exponential functions, are distinct from the exponential near-critical surface segregation profiles normally observed in small-molecule liquids beyond a molecular scale near the solid substrate [26]. Rounding of the critical-adsorption profile due to relative neutral fluid-wall interactions in mixtures (*i.e.*, "weak surface field") has recently been appreciated in theoretical modeling of critical adsorption using Ising models with interacting boundaries [27]. "Weak critical adsorption" has been observed in small molecule mixtures as well, when one of the compounds was varied in such a way that the relative fluid-substrate surface interactions are balanced [28]. We suggest that the prevalence of polymer-surface interaction screening in polymer layers, as for excluded-volume interactions in polymer melts, leads to a general propensity towards "weak critical adsorption" type compositional enrichment in confined polymer blend films.

In summary, we investigated the surface enrichment in polymer blend films close to the critical point for bulk phase separation as a function of film thickness and temperature. The measurements indicate a gradual transition from an in-plane phase separation in thinner films to a more layered morphology in thicker films. The thickness where this transition occurs is near 1200 Å and thus comparable to the spinodal wavelength L_{c}. This finding is in agreement with earlier suggestions based on AFM and optical-microscopy studies [10, 11]. The interplay of wetting, film thickness and interfacial tension corresponds to that observed in experiments with small binary mixtures confined between glass walls [29].

* * *

HG would like to thank the Alexander von Humboldt Foundation for financial support.

REFERENCES

[1] Debye P. and Cleland R., *J. Appl. Phys.*, **30** (1959) 843; Wiegand S., Berg R. F. and Sengers J. M. H. L., *J. Chem. Phys.*, **109** (1998) 4533.
[2] Grüll H. and Woermann D., *Ber. Bunsen. Phys. Chem.*, **101** (1997) 814; Beysens D. and Esteve D., *Phys. Rev. Lett.*, **54** (1985) 2123; Gallagher P. D. and Maher J. V., *Phys. Rev. A*, **46** (1992) 2012.
[3] Wypych G., *Handbook of Fillers*, 2nd edition (Plastic Design Library) 1999.
[4] Schmidt I. and Binder K., *J. Phys.*, **46** (1985) 1631.
[5] Diehl H. W., *Ber. Bunsen. Phys. Chem.*, **98** (1994) 466.
[6] Scheffold F., Eiser E., Budkowski A. *et al.*, *J. Chem. Phys.*, **104** (1996) 8786.
[7] Kerle T., Klein J. and Binder K., *Eur. Phys. J. B*, **7** (1999) 401; *Phys. Rev. Lett.*, **77** (1996) 1318.
[8] Krausch G., Dai C. A., Kramer E. J. *et al.*, *Macromolecules*, **26** (1993) 5566.
[9] Karim A., Slawecki T. M., Kumar S. K. *et al.*, *Macromolecules*, **31** (1998) 857.
[10] Sung L., Karim A., Douglas J. F. *et al.*, *Phys. Rev. Lett.*, **76** (1996) 4368.

[11] ERMI B. D., KARIM A. and DOUGLAS J. F., *J. Polym. Sci. B*, **36** (1998) 191.
[12] BINDER K., NIELABA P. and PEREYRA V., *Z. Phys. B*, **104** (1997) 81.
[13] GRÜLL H., SCHREYER A., MAJKRZAK C. F., BERK N. F. and HAN C. C., *Europhys. Lett.*, **50** (2000) 107.
[14] GRÜLL H., HAYASHI M., JINNAI H., HASHIMOTO T. and HAN C. C., unpublished data.
[15] FLORY P. J., *Principles of Polymer Chemistry* (Cornell University Press, Ithaca, NY) 1959.
[16] WELP K. A., CO C. C. and WOOL R. P., *J. Neutron Res.*, **8** (1999) 37.
[17] BURKHARDT T. W., *Phys. Rev. Lett.*, **48** (1982) 216.
[18] BRAY A. J. and MOORE M. A., *J. Phys. A*, **10** (1977) 1927.
[19] GRÜLL H. and WOERMANN D., *J. Chem. Phys.*, **105** (1996) 2527.
[20] WENDLANDT M., KERLE T., HEUBERGER M. and KLEIN J., *J. Polym. Sci. B*, **38** (2000) 831.
[21] JONES R. A. L., NORTON L. J., KRAMER E. J. *et al.*, *Europhys. Lett.*, **12** (1990) 41.
[22] NORTON L. J., KRAMER E. J., BATES F. S. *et al.*, *Macromolecules*, **28** (1995) 8621.
[23] ZINK F., KERLE T. and KLEIN J., *Macromolecules*, **31** (1998) 417.
[24] FREED K. F., *J. Chem. Phys.*, **105** (1996) 10572.
[25] HARIHARAN A., KUMAR S. K. and RUSSELL T. P., *Macromolecules*, **24** (1991) 4909.
[26] FISHER M. E. and DE GENNES P. G., *C. R. Acad. Sci. Ser. B*, **287** (1978) 207; CARPENTER J. H., LAW B. M. and SMITH D. S. P., *Phys. Rev. Lett.*, **59** (1999) 5655; LAW B. M., *Prog. Surf. Sci.*, **66** (2001) 161.
[27] CIACH A., MACIOLEK A. and STECKI J., *J. Chem. Phys.*, **108** (1998) 5913.
[28] HO J.-H. J. and LAW B. M., *Phys. Rev. Lett.*, **86** (2001) 2070.
[29] RATHKE B., GRÜLL H., GRADEWALD L. *et al.*, *Z. Phys. Chem.*, **199** (1997) 275; BODENSOHN J. and GOLDBURG W. I., *Phys. Rev. A*, **46** (1992) 5084.